Magento optical properties and structure of tellurite glasses modified by alkaline ions

A. M. Al-Syadi[a,b], M. Alfarh[c,d], H. Algarni[c,d], Mohammed S. Alqahtani[e,*], M. Reben[f], H. Afifi[g], El Sayed Yousef[c,d,h]

[a]*Department of Physics, Faculty of Science and Arts, Najran University, Saudi Arabia*

[b]*Department of Physics, Faculty of Education, Ibb University, Yemen.*

[c]*Physics Dep., Faculty of Science, King Khalid University, P. O. Box 9004, Abha, Saudi Arabia*

[d]*Research Center for Advanced Materials Science (RCAMS), King Khalid University, Postcode: 9004, Zip code: 61413, Abha, Saudi Arabia*

[e]*Department of Radiological Sciences, College of Applied Medical Sciences, King Khalid University, Abha 61421, Saudi Arabia*

[f]*Faculty of Materials Science and Ceramics, AGH – University of Science and Technology, al. Mickiewicza 30, 30-059 Cracow, Poland*

[g]*Ultarsonic Laboratory, National Institute for Standards, Tersa Street El-haram, El-Giza, P.O. Box 136, Code N 12211, Egypt*

[h]*Physics department, Faculty of Science, Al Azhar University, Assiut Branch, Egypt*

In this paper we prepared glasses with composition (75-x)TeO_2–5Nb_2O_5–20ZnO–xNa_2O mol%, (x = 7, 10, 15, and 18) were synthesized by using the conventional quench-melting method. The Faraday effect has been investigated as well as the structure of these glasses was analyzed by Raman spectroscopy. It can observe that when the Na_2O concentration increased from 7 to 18 mol%, the value of the Verdet constant decreased from 0.113 to 0.071 min/G.cm. This result can be interpreted as the following: when adding Na_2O into the glass matrix, leads to the attendance of non-bridging oxygens (NBO). The peak (d) in the range of 717–721 cm^{-1} is related to the stretching vibrations of Te-O^- and Te=O bonds containing nonbridging oxygen in TeO_3 (tp) phase.

(Received May 2, 2022; Accepted December 14, 2022)

Keywords: Raman, Structural, TeO_2–based glasses, Faraday effect, Magneto-optical properties, Verdet constant

1. Introduction

Due to their contribution to scientific and technical innovations, glasses used in high-tech applications have become a cutting-edge study area in materials science. As a result, much emphasis has been given to the study of various glass varieties that may be employed in many technical applications [1,2]. Tellurite glasses have attracted a lot of interest from scientists in the recent two decades. Tellurite glasses have proved to have extremely promising features in terms of satisfying optical application requirements, and they have a lot of promise for usage in amplifiers, switching devices, and laser technology [3]. Tellurite glasses have low phonon energy, a high refractive index, a high dielectric constant, and high infrared transmissivity, which provides them suitable matrices for amplifier mediums and laser hosts when compared to SiO_2, P_2O_5, B_2O_3, and GeO_2-based glass systems [1,3,4]. New TeO_2–based glasses have recently been developed as particularly appealing materials for optical amplifiers in a broad variety of wavelength division multiplexing (WDM) network systems [4,5]. Their low glass transition and melting temperatures, as well as their thermal and chemical stability and strong devitrification resistance, make them

* Corresponding author: mosalqhtani@kku.edu.sa
https://doi.org/10.15251/JOR.2022.186.805

easy to manufacture. [6–9]. Because of its broad glass-forming range and strong solubility of transition oxide elements [10], the addition of zinc to tellurite glass is of significant importance to glass technology and applications. Furthermore, ZnO in the glass structure raises the refractive index value and acts as a glass stabilizer [11,12]. The addition of Nb_2O_5 to TeO_2 results in a small domain, improved vitrification, and a higher refractive index [11,13]. The incorporation of Na_2O enhances thermal stability and the suitability of the ion-exchange process [9,14,15]. The addition of alkali oxides to tellurium oxides, such as Li_2O, Na_2O, and K_2O, may enhance toughness, glass-forming ability, and lower melting point while also increasing non-bridging oxygen (NBO) in the matrix [11,16]. As a result, to make tellurite glasses, Na_2O was chosen as a secondary component in this investigation. Nb_2O_5 also has magnetic and magneto-optical characteristics that are appealing to glass. For example, the high polarizability, high field strength, low photon energy, low bandgap, and diamagnetic character of Nb^{5+} ions [17] are very appealing to glass magnetic and Faraday Effect-based magneto-optical technology, which is gaining popularity in optical fiber sensors, isolators, and magneto-optical current transducers [18].

The transition metal oxides Nb^{3+}, Nb^{4+}, and Nb^{5+}, on the other hand, include Nb_2O_5. The unfilled outer shell of niobium causes paramagnetic behavior in the lower valence states, whereas the empty d shell (4d0) electron structure causes diamagnetic behavior in the Nb^{5+} ions. Glass containing Nb_2O_5 has high optical basicity, which may offer an oxidation environment for higher valence states of niobium, namely Nb^{5+}, and electron transfer between Nb^{5+} and O^{2-} [19]. Because Nb5+ has a high diamagnetic susceptibility (-9×10^{-6} emu/mol), it is predicted that its presence would enhance magnetization and the Verdet constant. Furthermore, the Nb^{5+} cation has a high charge and a moderate ionic radius of 0.69, resulting in strong ionic field strength and polarizability, both of which are advantageous to the magneto-optical characteristics of glass [20]. More potential for the tellurite glass family has recently been suggested, including the idea of using them to produce efficient diamagnetic magneto-optic fiber components that leverage the Faraday effect [21]. The Faraday effect relies on the magnetic field turning the plane of polarization of linearly polarized light in isotropic transparent materials [22]. Faraday rotation, or magneto-optical rotation of light polarization, is significant for a variety of applications, including optical isolators and optical diodes inside laser resonators [23]. The Verdet constant [24] determines the intensity of the Faraday Effect in a material. The Verdet constant's magnitude is determined by the gain medium host, the dopant and its concentration, the oscillation wavelength, and the temperature [23]. On the other hand, by doping highly polarized diamagnetic ions or creating surface Plasmon Resonance (SPR) effects, the Faraday rotation effect in diamagnetic glass may be enhanced [25].

The TeO_2–based glass system with the formula $(75\text{-}x)TeO_2–5Nb_2O_5–20ZnO–xNa_2O$ mol%, (x = 7, 10, 15, and 18), was synthesized in the present study utilizing the melt-quenching approach, which was less cost-effective and time-consuming. The Faraday effect was studied, and Raman spectroscopy was used to examine the structure of these glasses.

2. Experimental work

Using the traditional quench-melting procedure, glass systems with a composition of $(75\text{-}x)TeO_2–5Nb_2O_5–20ZnO–xNa_2O$ mol% (x = 7, 10, 15, and 18) were created. The raw materials were powdered and placed in a platinum crucible, which was heated in a melting furnace to 920°C for 45 minutes, with the melt being stirred occasionally. A graphite mold was used to cast the very viscous melt. The quenched samples were annealed at 340°C for 2 hours before being cooled to room temperature within the furnace. Table 1 shows the chemical composition of the TeO_2-based glass under investigation. Figure 1 shows a schematic diagram of the setup used to obtain the Verdet constants for various glasses. A tangential probe and a Tesla-meter were used to calibrate an electromagnet that creates a variable flux density up to 1 T and creates a variable flux density up to 1 T. The glass samples were placed in a magnetic field between two polarizers (input and output) that were 90 degrees apart. The intensity of the laser beam (= 632 nm) passing the glass and transmitted through the output polarizer was close to zero in the absence of a magnetic field. Visually and with a solar-photo detector, this could be determined. Due to the rotation of the plane

of polarization, which linearly dependent on the flux density B as shown in Fig. 1, a good percentage of laser intensity was transmitted through when the magnetic field was applied. An ocular and a protractor projected on the output polarizer were used to determine the amount and direction of rotation. The direction of the magnetizing current was reversed, and the rotation measurement was repeated, to attain high precision.

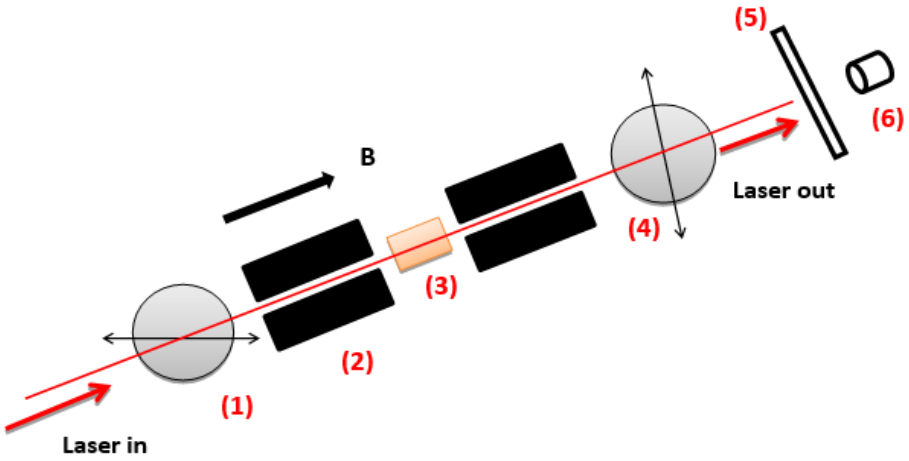

Fig. 1. (1) Input Polarizer, (2) Magnet Pole, (3) Glass Sample, (4) Output Polarizer, (5) Fluorescent Screen, (6) Ocular.

The Raman spectrometer (Senterra, Bruker GmbH, Germany) was used to investigate the structure of this tellurite glass at 514 nm excitation.

3. Results and discussion

Magneto-optical materials have been employed in a variety of photonics applications, most notably in the fabrication of optical isolators and diodes [26]. Optical isolation is achieved in such systems by modifying the propagation of light using an external magnetic field. By creating circular birefringence via the Faraday effect, the magnetic field modifies the optical response of the medium, resulting in a rotation of the plane of polarization of an incoming linearly polarized light beam [21,27]. The Verdet constant, V, is a characteristic property of the material that controls the amount of the Faraday effect. Zeeman splitting of atomic energy levels causes magneto-optical rotation of light polarization [24]. The left and right circularly polarised components of a linearly polarised laser beam would experience different refractive indices and hence propagate at different speeds in various directions of propagation through a magneto-optical material to which a magnetic field is applied. As a result, an incoming linearly polarised laser beam's plane of polarization will spin as it propagates through such a material [23]. The rotating angle of glass is linked to the magnetic field B, the Verdet constant (V), and the length L of glass in the following equation [28], according to Faraday rotation theory:

$$\theta = VLB \tag{1}$$

The relationship between the current and current-produced magnetic field indicated in Eq (2) [28] was analyzed to validate the self-constructed setup.

$$B = \frac{\mu_0 NI}{L_s} \tag{2}$$

where μ_0 is a constant of 1.26×10^{-6} Hm^{-1}, N is the number of turns in the coil that surrounding the solenoids, I is the current that flows through the solenoids, and Ls is the length of the solenoids As

demonstrated in Fig. 2, the current and magnetic field had a linear relationship, showing that the solenoid was stable.

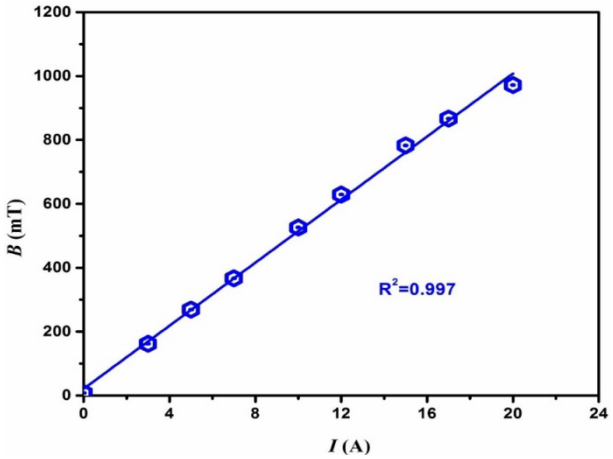

Fig. 2. Relation between the current (I) and magnetic field (B).

Fig. 3 (a-d) shows the θ of samples with fixed length L as a function of magnetic field B, it can be that all samples appear the θ increased with the increase of B. The slope indicates to Verdet constant (V) that is calculated by (slope = VL). The values of the Verdet constant (at λ=632 nm) for samples are listed in Table 1.

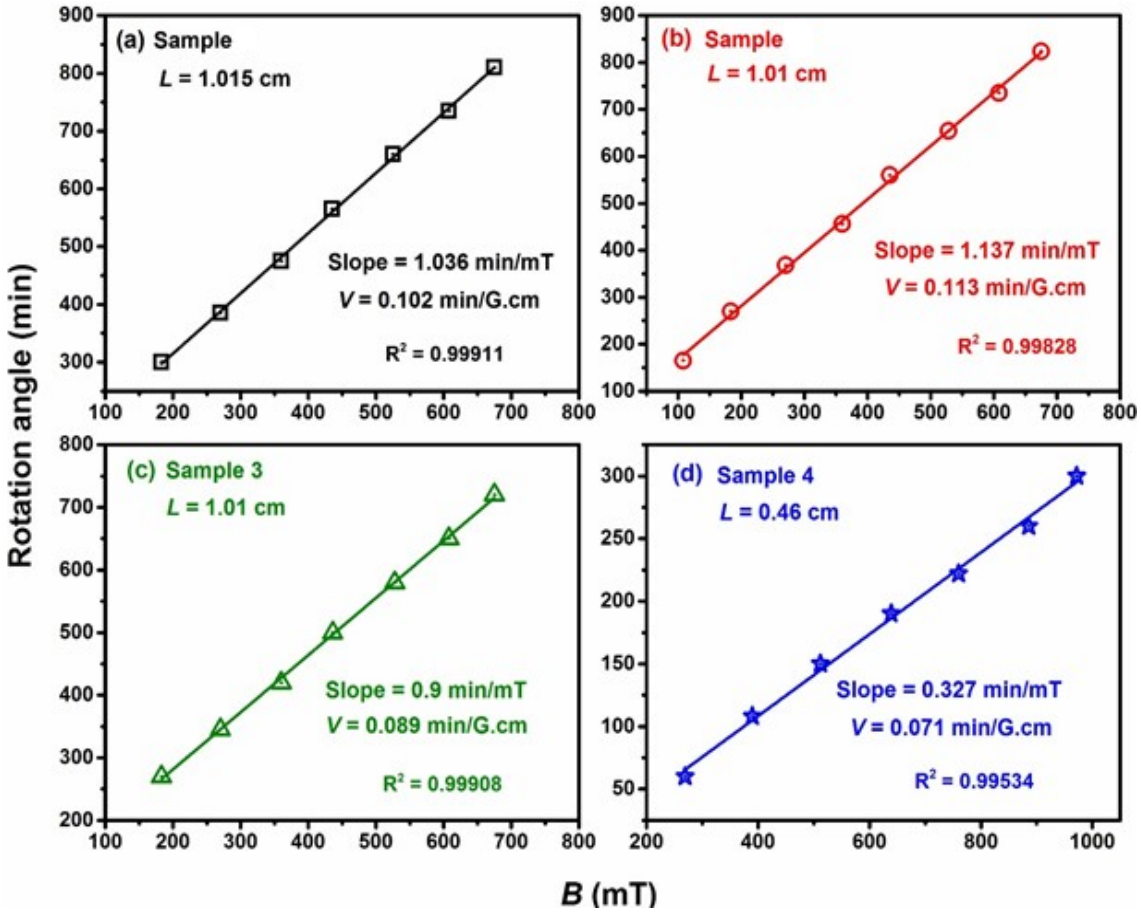

Fig. 3. Relation between magnetic field B and Faraday rotation angle θ for the TeO_2–based glasses (75-x)TeO_2–5Nb_2O_5–20ZnO–xNa_2O mol%: (a) x=7; (b) x=10; (c) x=15 and (d) x=18.

Table 1. The Verdet constant (V) at λ = 632 nm of the TeO_2–based glasses [(75-x)TeO_2– 5Nb_2O_5–20ZnO–xNa_2O mol%].

Sample code	Composition in mol%	Verdet constant *V*(min/G.cm)
Sample 1	68TeO_2–5Nb_2O_5–20ZnO–7Na_2O	0.113
Sample 2	65TeO_2–5Nb_2O_5–20ZnO–10Na_2O	0.102
Sample 3	60TeO_2–5Nb_2O_5–20ZnO–15Na_2O	0.089
Sample 4	57TeO_2–5Nb_2O_5–20ZnO–18Na_2O	0.071

These Verdet constant values are in excellent accord with earlier publications [1,20,28], however, the findings from these glasses were better than those published in the literature [29]. The Faraday Effect experiments were able to detect the phenomena of light twisting its plane of polarization under the influence of a longitudinal magnetic field in all of the studied glasses. Due to the diamagnetic nature of Nb^{5+} ions and high diamagnetic susceptibility, high Verdet constant values in these glasses are ascribed to the presence of Nb_2O_5 [17,20]. The high optical basicity of glass containing Nb_2O_5 may also offer an oxidation environment for higher valence states of niobium, such as Nb^{5+}, and electron transfer between Nb^{5+} and O^{2-} [19]. As a result, the presence of Nb^{5+} is predicted to boost magnetization and the Verdet constant.

Figure 4 shows the Verdet constant values of the as-prepared glasses as a function of Na_2O concentration. It can be shown that when the concentration of Na2O increased from 7 to 18 mol%, the Verdet constant reduced from 0.113 to 0.071 min/G.cm. The following is how this result might be interpreted: When Na_2O is added to the glass matrix, it causes non-bridging oxygens to appear (NBO). The number of NBOs increases as the concentration of Na_2O increases, making electron transmission in the glass greater. As a result of the electron transport through glass, the Verdet constant is growing [20]. Furthermore, the Verdet constant decreases with increasing Na_2O concentration, which might be due to the substantial increase in distance between atoms/molecules, which is inversely proportional to the Verdet constant, as indicated in Eq. (3): [28]

$$V = \frac{-3(\alpha_{O2-})^2 I}{4r^6} \tag{3}$$

where *r* is the distance between the atoms/molecules, *I* is the first ionization energy of the atom, and (α_{O2}-) is glass polarizability**.**

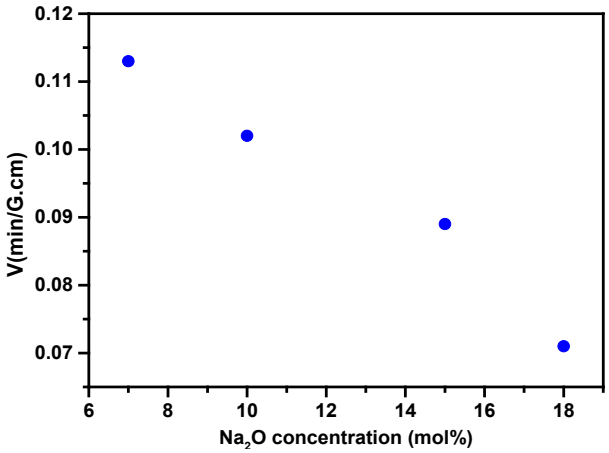

Fig. 4. Verdet constants of the TeO_2–based glasses (75-x)TeO_2–5Nb_2O_5–20ZnO–xNa_2O mol% as a function of Na_2O concentration.

The Raman spectrum is a useful tool for investigating the structure of glass materials. Figure 5 shows the Raman spectra of the as-prepared glasses from 300 to 880 cm^{-1}. The disordered

features in these glasses are primarily responsible for two large scattering peaks. According to each structural unit in the glass network, which was represented as (a-e) bands, the spectra of glass samples 1 and 2 were deconvoluted into five separate Gaussian peaks. However, the spectra of glass samples 3 and 4 were deconvoluted into three separate Gaussian peaks, one for each structural unit in the glass network, which were represented as (a, c, and e) bands.

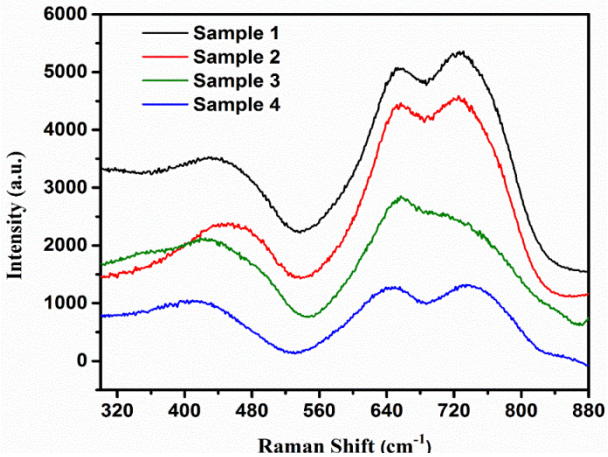

Fig. 5. Raman spectra of the as-prepared glasses.

Figure 6(a-d) depicts those bands, which are listed in Table 2. Table 3 also included their band assignments. The addition of modifier oxide to TeO_2 rich glass weakened the axial Te-O connections and opened the glass network. As a result, the TeO_4 phase unit (tbp) is converted to TeO_{3+1} and TeO_3 (tp) phases [30]. For symmetrical stretching or bending vibrations of Te-O-Te links [31,32] and symmetric stretching vibrations of the Zn–O bond in the ZnO_4 tetrahedral group [30, 33], the band (a) in the spectral range 431- 462 cm^{-1} has been determined. The anti-symmetrical stretching of the continuous network formed of TeO_4 (tbp) trigonal bipyramidal units is specified by the band (b) that emerged in the range 582-592 cm1 [34,35,36]. The symmetric stretching vibrations of tellurium and axial oxygen (Te) in $Te_{qe}O_{ax}TeO_4$ (tbp) units are attributed to the band (c) at 640–654 cm^{-1} [37, 38]. The stretching vibrations of TeO and Te=O bonds including nonbridging oxygen in TeO_3 (tp) phase were connected to the peak (d) in the range of 717–721 cm^{-1} [36]. Finally, stretching vibrations of TeO_3/TeO_{3+1} units are verified in the band designated (e) in the range 733–773 cm^{-1} [32,34,39,40].

Table 2. The band center of de-convolution of the Raman spectra of studied glasses.

Sample code	Band a	Band b	Band c	Band d	Band e
Sample 1	455	582	654	717	761
Sample 2	462	591	651	721	773
Sample 3	455	-	643	-	733
Sample 4	431	-	640	-	747

Table 3. Peak assignments for the as-prepared glasses.

Raman shift (cm^{-1})	Vibrational modes	Ref.
431-462	Symmetrical stretching or bending vibrations of Te-O-Te linkages and symmetric stretching vibration of ZnO_4 tetrahedral unit.	[30,31,32,33]
582-592	Anti-symmetrical stretching of the continuous network composed of TeO_4 tbp.	[34,35,36]
640-654	Symmetric stretching vibrations of tellurium and axial oxygen (Te) in Te_{qe}-O_{ax}-TeO_4 (tbp) trigonal bipyramidal units.	[37,38]
717-721	Stretching vibrations of Te-O^- and Te=O bonds containing nonbridging oxygen in TeO_3 tp.	[36]
733-773	Stretching vibrations of TeO_3/TeO_{3+1} units.	[32,34,39,40]

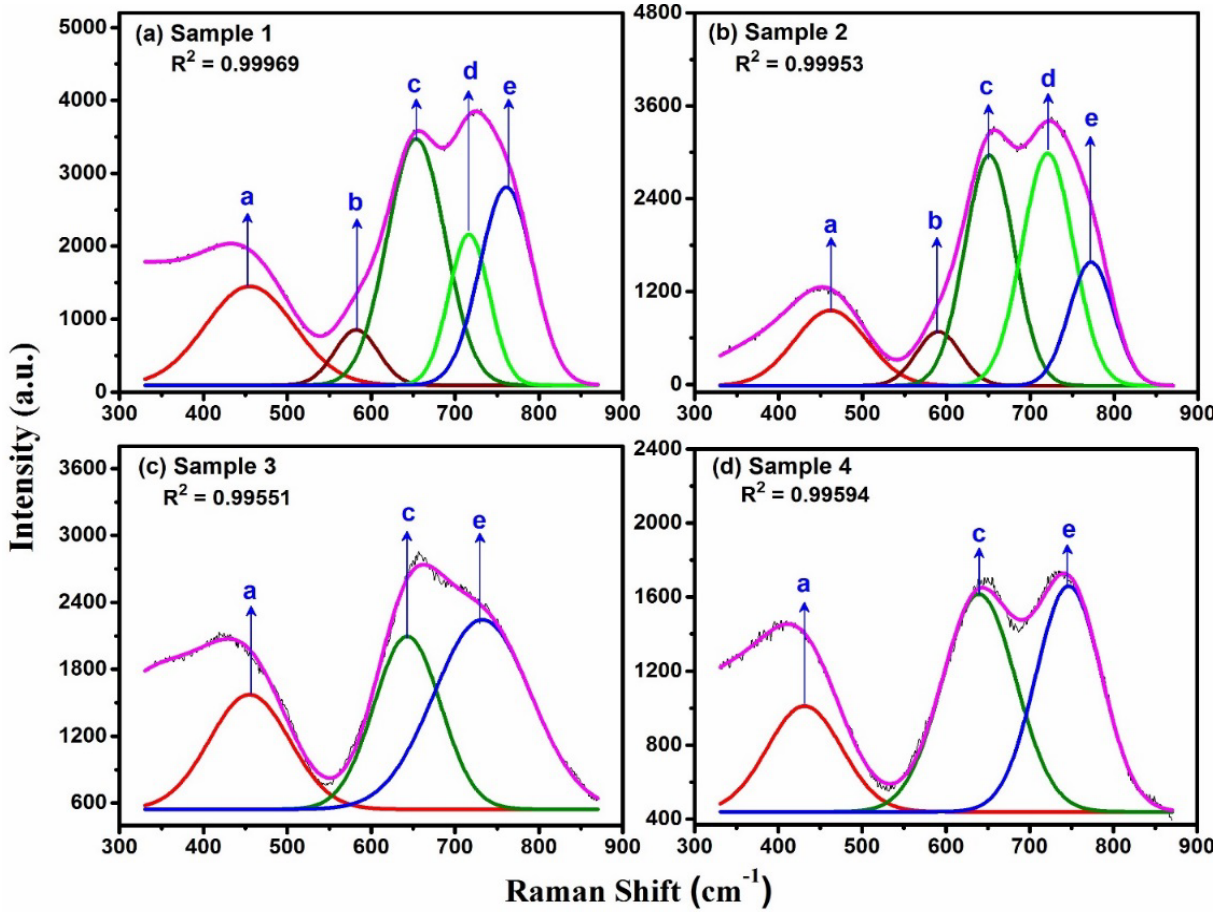

Fig. 6. Raman spectra and curve-fitting of the TeO_2–based glasses (75-x)TeO_2–5Nb_2O_5–20ZnO–xNa_2O mol%: (a) x=7; (b) x=10; (c) x=15 and (d) x=18.

4. Conclusion

The incorporated Na_2O to the tellurite glasses with composition TeO_2–Nb_2O_5–ZnO leads to a decrease in the Verdet constant. The glass $68TeO_2$–$5Nb_2O_5$–20ZnO–$7Na_2O$ has the highest value (V= 0.113 min/G.cm) otherwise the glass $57TeO_2$–$5Nb_2O_5$–20ZnO–$18Na_2O$ has the lowest value (V= 0.071 min/G.cm). The Na_2O creates non-bridging oxygens (NBO) in the present glasses. Hence the Verdet constant increase with increase NBO. These Verdet constant values are excellent compared with tellurite glasses published before. Symmetric stretching vibrations of Te_{qe}-O_{ax}-TeO_4 (tbp) trigonal bipyramidal units appeared at 640-654 cm^{-1}.

Acknowledgments

This work was the support of King Khalid University, the Ministry of Education, and the Kingdom of Saudi Arabia for this research through a grant (RCAMS/KKU/004/21) under the research center for advanced material science. Also, the authors are thankful to the Deanship of Scientific Research at Najran University for funding this work under the Research Collaboration Funding program grant code (NU/RC/MRC/11/3)

References

[1] K. Pach-Zawada, E. Golis, P. Pawlik, K. Kotynia, R. Miedziński, J. Filipecki, Physica B: Condensed Matter 562 (2019) 36-41; https://doi.org/10.1016/j.physb.2019.03.008

[2] A. Jha, S. Shen, M. Naftaly, Phys. Rev. 62 (2000) 6215-6227; https://doi.org/10.1103/PhysRevB.62.6215

[3] K.B. Kavaklıoğlu, S. Aydin, M. Çelikbilek, A.E. Ersundu, International Journal of Applied Glass Science 6, (2015) 406-418; https://doi.org/10.1111/ijag.12103

[4] M. El-Okr, M. Ibrahem, M Farouk, Journal of Physics & Chemistry of Solids 69 (2008) 2564; https://doi.org/10.1016/j.jpcs.2008.05.015

[5] El S. Yousef, M.M. Elokr, Y.M. Aboudeif, Chalcogenide Letters 12 (2015) 597-607.

[6] B. Burtan-Gwizdala, M. Reben, J. Cisowski, S. Szpil, R. Lisiecki, I. Grelowska, Optical Materials, 107 (2020) 109968; https://doi.org/10.1016/j.optmat.2020.109968

[7] Y.S. Rammah, I.O. Olarinoye, F.I. El-Agawany, A. El-Adawy, A. Gamal, Ceramics International 46 (2020) 25440-25452; https://doi.org/10.1016/j.ceramint.2020.07.014

[8] R.A.H. El-Mallawany, Tellurite Glasses Handbook, CRC Press, Boca Raton, London, New York, Washington, DC, 2002.

[9] M. Çelikbilek, A.E. Ersundu, S. Aydin, J. Am. Ceram. Soc. 96 (2013) 1470-1476; https://doi.org/10.1111/jace.12335

[10] W. Huaxin, P. Zhang, Z. Zang, Appl. Phys. Lett. 116 (2020) 162103; https://doi.org/10.1063/5.0005464

[11] N. Elkhoshkhany, R. Essam, Journal of Non-Crystalline Solids 536 (2020) 119994; https://doi.org/10.1016/j.jnoncrysol.2020.119994

[12] M.F. Faznny, M.K. Halimah, M.N. Azlan, J. Optoelectr. Biomed. Mater. 8 (2016) 49-59.

[13] A. Faeghinia, R. Nemati, M. Sheikhani, Int. J. Mater. Mechan. Manuf. 5 (February 2017); https://doi.org/10.18178/ijmmm.2017.5.1.282

[14] K.B. Kavaklıoğlu, M. Çelikbilek, A.E. Ersundu, S. Aydin, pp. 237-42 in Materials Science and Technology Conference and Exhibition Proceedings, Vol. 1, Edited by J. Du and J. Kieffer, Pittsburgh, PA, 2012

[15] J. Heo, D. Lam, G.H. Sigel Jr., E.A. Mendoza, A.D. Hensley, J. Am. Ceram. Soc., 75 (1992) 77-81; https://doi.org/10.1111/j.1151-2916.1992.tb08176.x

[16] M.A. Sidkey, M.S. Gaafar, Phys. B 348 (2004) 46-55;

https://doi.org/10.1016/j.physb.2003.11.005
[17] K. Nisa, E. Ahmed, J. Appl. Phys. 3 (2013) 80-87; https://doi.org/10.9790/4861-0358087
[18] J. Zubia, L. Casado, G. Aldabaldetreku, A. Montero, Sensors 13 (2013) 13584-13595; https://doi.org/10.3390/s131013584
[19] V. Dimitrov, T. Komatsu, J. Univ. Chem. Technol. Metal. 45 (2010) 219-250.
[20] Q. Chen, Journal of Non-Crystalline Solids 519 (2019) 119451; https://doi.org/10.1016/j.jnoncrysol.2019.05.027
[21] M.A. Schmidt, L. Wondraczek, H.W. Lee, N. Granzow, N. Da, P.St.J. Russell, Advanced Materials 23 (2011) 2681-2688; https://doi.org/10.1002/adma.201100364
[22] E.P. Golis, A. Ingram, Journal of Physics, Conference Series, 79 (2007) 012003-012003; https://doi.org/10.1088/1742-6596/79/1/012003
[23] L. Harris, D. Ottaway, P.J. Veitch, Appl Phys B 106 (2012) 429-433; https://doi.org/10.1007/s00340-011-4761-3
[24] M.N. Deeter, G.W. Day, A.H. Rose, in M.J. Weber (ed.) CRC Handbook of Laser Science and Technology, Supplement 2: Optical Materials (CRC Press, Boca Raton, 1994), Sect. 9
[25] K.J. Prashant, Y. Xiao, Nano letter 9 (2009) 1644-1650; https://doi.org/10.1021/nl900007k
[26] A.K. Zvezdin, V.A. Kotov, Modern Magnetooptics and Magnetooptical Materials, Taylor & Francis Group, New York 1997; https://doi.org/10.1201/9780367802608
[27] J.M. Liu, Photonic Devices, Cambridge University Press, Cambridge 2005.
[28] Q. Chen, Journal of Alloys and Compounds 828 (2020) 154448; https://doi.org/10.1016/j.jallcom.2020.154448
[29] M. Elisa, L. Boroica, B.A. Sava, S.M. Iordache, A.M. Iordache, I.C. Vasiliu, R.C. Stefan, A.C. Galca, V. Kuncser, M. Eftimie, Journal of the American Ceramic Society 103 (2020) 3978-3990; https://doi.org/10.1111/jace.17071
[30] S.K. Ahmmad, M.A. Samee, S.M. Taqiullah, Syed Rahman, J. Taibah Univ. Sci. 10 (2016) 329-339; https://doi.org/10.1016/j.jtusci.2014.12.008
[31] V. Kamalaker, G. Upender, Ch. Ramesh, V. Chandra Mouli, Spectrochimica Acta Part A 89 (2012) 149- 154; https://doi.org/10.1016/j.saa.2011.12.057
[32] A. Kaur, A. Khanna , V.G. Sathe, F. Gonzalez, B. Ortiz, Phase Transitions 86 (2013) 598-619; https://doi.org/10.1080/01411594.2012.727998
[33] S.F. Mansour, M.Y. Hassaan, A.M. Emara, Sol. State Sci. 37 (2014) 33-39; https://doi.org/10.1016/j.solidstatesciences.2014.08.004
[34] A. Kaur, A. Khanna, AIP Conference Proceedings 2115 (2019) 030253; https://doi.org/10.1063/1.5113092
[35] El S. Yousef, H.H. Hegazy , M.M. Elokr , Y.M. Aboudeif, Chalcogenide Letters 12 (2015)653 - 663.
[36] S.F. Mansour, El Sayed Yousef , M.Y. Hassaan , A.M. Emara, Solid State Sciences 37 (2014) 33-39; https://doi.org/10.1016/j.solidstatesciences.2014.08.004
[37] El Sayed Yousef, S.F. Mansour, M.Y. Hassaan, A.M. Emara, Optik 127 (2016) 8933-8939; https://doi.org/10.1016/j.ijleo.2016.06.113
[38] J. Lin , W. Huang, Z. Sun, C.S. Ray , D.E. Day, Journal of Non-Crystalline Solids 336 (2004) 189-194; https://doi.org/10.1016/j.jnoncrysol.2004.02.007
[39] G. Upender , S. Ramesh , M. Prasad, V.G. Sathe, V.C. Mouli, Journal of Alloys and Compounds 504 (2010) 468-474; https://doi.org/10.1016/j.jallcom.2010.06.006
[40] H. Fares, I. Jlassi, H. Elhouichet, M. Férid, Journal of Non-Crystalline Solids 396-397 (2014) 1-7; https://doi.org/10.1016/j.jnoncrysol.2014.04.012